Self-Calibrating Depth from Refraction

Zhihu Chen[1], Kwan-Yee K. Wong[1], Yasuyuki Matsushita[2], Xiaolong Zhu[1], and Miaomiao Liu[1]

[1] Department of Computer Science, The University of Hong Kong, Hong Kong
[2] Microsoft Research Asia, Beijing, P.R.China

Abstract

In this paper, we introduce a novel method for depth acquisition based on refraction of light. A scene is captured twice by a fixed perspective camera, with the first image captured directly by the camera and the second by placing a transparent medium between the scene and the camera. A depth map of the scene is then recovered from the displacements of scene points in the images. Unlike other existing depth from refraction methods, our method does not require the knowledge of the pose and refractive index of the transparent medium, but can recover them directly from the input images. We hence call our method self-calibrating depth from refraction*. Experimental results on both synthetic and real-world data are presented, which demonstrate the effectiveness of the proposed method.*

1. Introduction

Depth from refraction is a depth acquisition method based on refraction of light. A scene is captured several times by a fixed perspective camera, with the first image captured directly by the camera and the others by placing a transparent medium between the scene and the camera. The depths of the scene points are then recovered from their displacements in the images.

Depth from refraction approach has various advantages over other existing 3D reconstruction approaches. First, unlike multi-view stereo methods, it does not require calibrating the relative rotations and translations of the camera as the viewpoint is fixed. Besides, a fixed viewpoint also makes the correspondence-problem much easier as the projections of a 3D point remain similar across images. Second, unlike depth from defocus methods which require expensive lenses with large apertures to improve depth sensitivity, the accuracy of depth from refraction can be improved by either 1) increasing the thickness of the refractive medium; 2) using a medium with a large refractive index; or 3) increasing the angle between the viewing direction of a 3D point and the surface normal of the medium. Third, unlike depth from diffusion methods, which require placing a diffuser with a known orientation close to the object being measured, depth from refraction allows the transparent medium being placed flexibly between the scene and the camera.

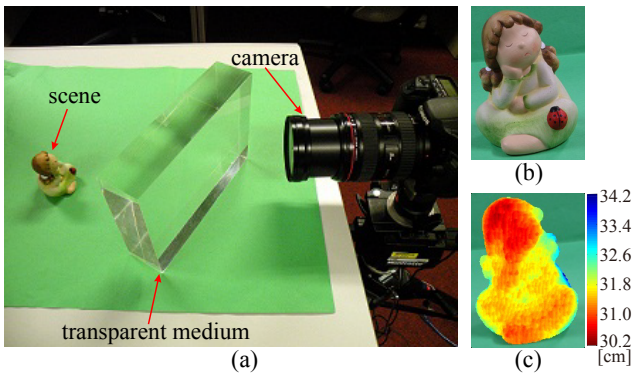

Figure 1. (a) Experimental setup; (b) a direct image of the scene; (c) reconstructed depth map of the scene.

Existing depth from refraction methods often require elaborate setup and pre-calibration for accurately knowing the pose and refractive index of the transparent medium. These greatly prohibit the applicability of the approach. In this paper, we introduce a novel method for depth from refraction which is more usable in various scenarios. Our method requires neither a careful hardware setup nor any pre-calibration. By simply putting a transparent medium between a camera and the scene, our method automatically estimates the pose and refractive index of the transparent medium as well as a depth map of the scene.

In our method, a scene is captured twice by a fixed perspective camera, with the first image (referred to as the direct image) captured directly by the camera and the second (referred to as the refracted image) by placing a transparent medium with two parallel planar faces between the scene and the camera (see Fig. 1). By analyzing the displacements of the scene points in the images, we derive a closed form solution for recovering both the pose of the transparent medium and the depths of the scene points. Given a

third image captured with the transparent medium placed in a different pose, we further derive a closed form solution for recovering also the refractive index of the medium. We call our proposed method *self-calibrating depth from refraction* since it directly exploits information obtained from the images of the scene to determine the necessary parameters for estimating scene depth.

1.1. Related work

Depth acquisition has a long history in computer vision. Based on the number of viewpoints required, existing methods can be broadly classified into multi-view and multi-exposure approaches. Multi-view methods exploit stereo information to recover the depth of a scene [13]. The location of a 3D point can be estimated by finding and triangulating correspondences across images.

Instead of moving the camera to change the viewpoints, multi-exposure methods record the scene by changing the imaging process. Depth from defocus methods obtain depth by exploiting the fact that depth information is contained in an image taken with a limited field of depth: objects at a particular distance are focused in the image, while objects at other distances are blurred by different degrees depending on their distances. Pentland estimated a depth map of a scene by measuring the degree of defocus using one or two images [12]. In [17], Subbarao and Gurumoorthy proposed a simpler and more general method to recover depth by measuring the degree of blur of an edge. Surya and Subbarao [18] used simple local operations on two images taken by cameras with different aperture diameters for determining depth. Zhou *et al*. [20] pointed out that the accuracy of depth is restricted by the use of a circular aperture. They proposed a comprehensive framework to obtain an optimized pair of apertures. All the aforementioned methods require large apertures to improve depth sensitivity. Recently, Zhou *et al*. [19] proposed a depth from diffusion method. Their method requires placing a diffuser with known orientation near the scene. They showed that while depth from diffusion is similar in principle to depth from defocus, it can improve the accuracy of depth obtained with a small lens by increasing the diffusion angle of a diffuser.

Our work is more closely related to [6, 9, 3, 4, 14, 15]. In [6], Lee and Kweon obtained the geometry of an object using a transparent biprism. In [9] and [3], the authors estimated the depth of a scene using a transparent planar plate with 2 opposite faces being parallel to the image plane. In [4], Gao and Ahuja considered the case where the faces of the transparent medium are not parallel to the image plane, and images are captured by rotating the medium about the principal axis of the camera. They estimated the pose and the refractive index of the medium in an extra step using a calibration pattern. In [14, 15], Shimizu and Okutomi proposed *reflection stereo* which records the scene from a fixed viewpoint with and without the reflection light paths. The two light paths create individual images, and from these images, their method estimates depth by triangulation. Their setup uses either reflective or refractive medium for the implementation. However, their method requires a complex calibration setup as described in [16]. Our method as well uses a transparent plane-parallel medium; however, unlike the aforementioned methods, our method requires neither the medium plane being parallel to the image plane, nor a careful calibration of the pose and refractive index of the medium using a calibration pattern.

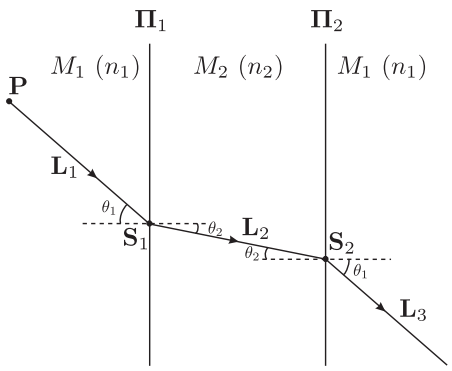

Figure 2. When a light ray passes from one medium to another with different speeds, it bends according to Snell's law. This phenomenon is known as refraction of light.

Shape recovery of transparent objects (also referred to as refractive objects) has also attracted the attentions of many researchers [11, 1, 10] recently. Instead of targeting at reconstructing refractive surfaces, this paper, on the other hand, exploits a refractive object to obtain the depth of a scene.

The rest of the paper is organized as follows. Section 2 briefly reviews the theory on refraction of light. Section 3 describes our proposed self-calibrating depth from refraction method in detail. Experimental results on both synthetic and real data are presented in Section 4, followed by conclusions in Section 5.

2. Refraction of Light

Refraction of light refers to the change in the direction of a light ray due to a change in its speed. This is commonly observed when a light ray passes from one medium to another (*e.g*., from air to water). The *refractive index* of a medium is defined as the ratio of the velocity of light in vacuum to the velocity of light in the said medium. Consider a light ray $\mathbf{L}_1$ originated from a point $\mathbf{P}$ passing from a medium M_1 to another medium M_2 (see Fig. 2). Let the refractive indices of M_1 and M_2 be n_1 and n_2 respectively, and the interface between the two media be a plane denoted by $\mathbf{\Pi}_1$. Suppose $\mathbf{L}_1$ intersects $\mathbf{\Pi}_1$ at $\mathbf{S}_1$ with an angle of incidence θ_1. After entering M_2, $\mathbf{L}_1$ changes it direction

and results in a refracted ray $\mathbf{L}_2$ with an angle of refraction θ_2. By Snell's law, the incident ray $\mathbf{L}_1$, the surface normal at $\mathbf{S}_1$ and the refracted ray $\mathbf{L}_2$ are coplanar, and the angle of incidence θ_1 and the angle of refraction θ_2 are related by

$$n_1 \sin\theta_1 = n_2 \sin\theta_2. \tag{1}$$

After travelling for some distance in M_2, $\mathbf{L}_2$ leaves M_2 and enters M_1 again. Let the interface between M_2 and M_1 be a plane denoted by $\mathbf{\Pi}_2$ which is parallel to $\mathbf{\Pi}_1$. Suppose $\mathbf{L}_2$ intersects $\mathbf{\Pi}_2$ at $\mathbf{S}_2$ and after entering M_1, it changes its direction and results in a refracted ray $\mathbf{L}_3$. Since $\mathbf{\Pi}_1$ and $\mathbf{\Pi}_2$ are parallel, it is easy to see that the angle of incidence for $\mathbf{L}_2$ is θ_2. It follows from Snell's law that the angle of refraction for $\mathbf{L}_3$ is θ_1, and $\mathbf{L}_1$, $\mathbf{L}_2$, $\mathbf{L}_3$ and the surface normals of $\mathbf{\Pi}_1$ and $\mathbf{\Pi}_2$ are coplanar, with $\mathbf{L}_1$ parallel to $\mathbf{L}_3$. Hence, the refraction plane of $\mathbf{P}$ (formed by $\mathbf{L}_1$, $\mathbf{L}_2$ and $\mathbf{L}_3$) is perpendicular to both $\mathbf{\Pi}_1$ and $\mathbf{\Pi}_2$.

It is worth noting that *total internal reflection* might happen when a light ray passes from a medium with a higher refractive index to one with a lower refractive index. The *critical angle* is defined as the angle of incidence that results in an angle of refraction being $90°$. When the angle of incidence is greater than the critical angle, total internal reflection occurs and the light ray does not cross the interface between the two media but is reflected totally back in the original medium.

3. Depth from Refraction

In this section, we will derive a closed form solution for recovering the depth of a scene from the displacements of scene points observed in two images due to refraction of light. As mentioned in Section 1, a scene will be captured twice by a fixed perspective camera, with the first image (referred to as the direct image) captured directly by the camera and the second (referred to as the refracted image) by placing a transparent medium between the scene and the camera. We assume the intrinsic parameters of the camera are known, and the transparent medium consists of two parallel planar faces through which light rays originate from scene points enter and leave the medium before reaching the camera.

3.1. Medium Surface ∥ Image Plane

Consider a 3D point $\mathbf{P}$ being observed by a camera centered at $\mathbf{O}$ (see Fig. 3). Let the projection of $\mathbf{P}$ on the image plane be a point $\mathbf{I}$. Suppose now a transparent medium M with two parallel planar faces is placed between $\mathbf{P}$ and the camera in such a way that the two parallel planar faces are parallel to the image plane. Due to refraction of light, $\mathbf{P}$ will no longer project to $\mathbf{I}$. Let $\mathbf{I}'$ be the new image position for the projection of $\mathbf{P}$. By considering the orthogonal

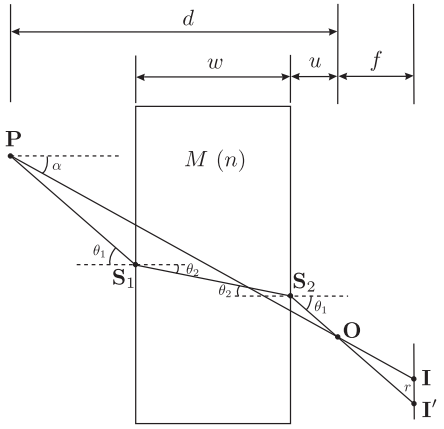

Figure 3. Special case of shape from refraction in which the parallel planar faces of the medium are parallel to the image plane. The depth of a 3D point can be recovered in closed form.

projection of the line $\mathbf{OP}$ on the image plane, we have

$$d\tan\alpha = (d - w - u)\tan\theta_1 + w\tan\theta_2 + u\tan\theta_1, \tag{2}$$

where d is the depth of $\mathbf{P}$, α is the angle between the visual ray of $\mathbf{P}$ and the principal axis of the camera (also referred to as the *viewing angle* of $\mathbf{P}$), w is the thickness of the medium M, u is the shortest distance between $\mathbf{O}$ and M, and θ_1 and θ_2 are the angle of incidence/refraction and angle of refraction/incidence as the ray originated from $\mathbf{P}$ enters/leaves M. Rearranging Eq. (2) gives

$$d = w\frac{\tan\theta_1 - \tan\theta_2}{\tan\theta_1 - \tan\alpha}. \tag{3}$$

By Snell's law, we have

$$\sin\theta_1 = n\sin\theta_2, \tag{4}$$

where n is the refractive index of M and the refractive index of the air can be approximated to one. Let r be the distance between $\mathbf{I}$ and $\mathbf{I}'$. It can be expressed in terms of the focal length f of the camera and the angles θ_1 and α as

$$r = f(\tan\theta_1 - \tan\alpha). \tag{5}$$

From Eq. (4) and Eq. (5), we derive expressions for $\tan\theta_1$ and $\tan\theta_2$ as

$$\tan\theta_1 = \frac{r}{f} + \tan\alpha, \tag{6}$$

$$\tan\theta_2 = \sqrt{\frac{\tan^2\theta_1}{n^2 + (n^2-1)\tan^2\theta_1}}. \tag{7}$$

Finally, substituting Eq. (6) and Eq. (7) into Eq. (3) gives

$$d = w\left(1 + \frac{f}{r}\tan\alpha\right)\left(1 - \sqrt{\frac{1}{n^2 + (n^2-1)(\frac{r}{f} + \tan\alpha)^2}}\right). \tag{8}$$

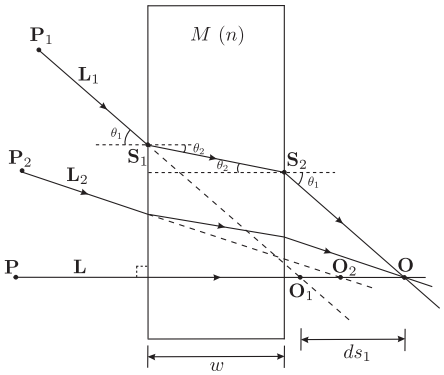

Figure 4. The formation process of the refracted image cannot be described by a simple pinhole camera model.

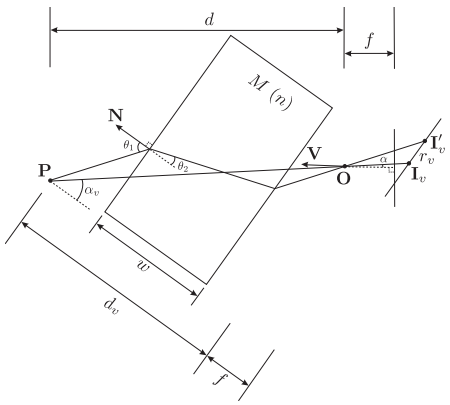

Figure 5. When the parallel planar faces of the medium are not parallel to the image plane, the depth of a 3D point can be recovered in closed form if the orientation of the medium is known.

From Eq. (8), it can be seen that d does not depend on u. This is very important in practice as it implies that the depth of a scene point can be recovered without knowing the distance between the medium M and the camera.

The proposed depth from refraction method has a major difference with traditional multi-view approaches as the formation process of the refracted image cannot be described by a simple pinhole camera model. In Fig. 4, $\mathbf{L}$ is a light ray originated from a point $\mathbf{P}$ to the camera center $\mathbf{O}$, and $\mathbf{L}$ is perpendicular to the medium surface. Light ray $\mathbf{L}_1$ originated from $\mathbf{P}_1$ intersects $\mathbf{L}$ at point $\mathbf{O}_1$, while light ray $\mathbf{L}_2$ originated from point $\mathbf{P}_2$ intersects $\mathbf{L}$ at point $\mathbf{O}_2$. The distance between $\mathbf{O}$ and $\mathbf{O}_1$ is given by

$$ds_1 = w - w\frac{\tan\theta_2}{\tan\theta_1} = w\left(1 - \frac{\sqrt{1-\sin^2\theta_1}}{\sqrt{n^2-\sin^2\theta_1}}\right). \quad (9)$$

From Eq. (9), it can be seen that ds_1 depends on θ_1. Therefore $\mathbf{O}_1$ and $\mathbf{O}_2$ are two different points. It follows that the formation process of the refracted image cannot be described by a simple pinhole camera model.

It has been pointed out in Section 2 that total internal reflection can only happen when a light ray passes from one medium with a higher refractive index to one with a lower index. In our setup, light rays travel through a composite air-glass-air medium. Total internal reflection should not occur when a light ray enters the glass from air as its speed in air is faster than its speed in glass. Since total internal reflection does not occur when the light ray enters the glass, the incident angle must be less than the critical angle when it re-enters air from the glass. Hence total internal reflection should never occur in our setup.

3.2. Medium Surface $\nparallel$ Image Plane

It has been shown in the previous subsection that depth can be recovered using Eq. (8) when the parallel planar faces of the transparent medium are parallel to the image plane. However, this proposed setup has two major limitations. First, it is difficult to ensure that the parallel planar faces of the medium are parallel to the image plane. Second, the depths of those 3D points whose viewing angles are small will be very sensitive to noises (see Fig. 7 (a)). As a result, only points with large viewing angles (*i.e.*, those projected near the border of the image) can be accurately recovered. In this subsection, we will show how the closed form solution derived under the special case can be applied to recover depth in the general case where the parallel planar faces of the medium are not parallel to the image plane but have a known orientation.

Suppose the surface normal of the parallel planar faces of the medium is given by the unit vector $\mathbf{N}$, and the viewing direction of the camera is given by the unit vector $\mathbf{V}$ (see Fig. 5). A rotation about the optical center of the camera, with a rotation axis given by the cross product of $\mathbf{V}$ and $\mathbf{N}$ and a rotation angle given by the angle between $\mathbf{V}$ and $\mathbf{N}$, will bring the image plane parallel to the parallel planar faces of the medium. Such a rotation will induce a planar homography that can transform the image of the original camera to an image observed by the camera after rotation. The closed form solution derived in the previous subsection can then be applied to the transformed image to recover the depth d_{v} of a point $\mathbf{P}$ with respect to the rotated camera using the viewing angle α_{v} of $\mathbf{P}$ and the displacement r_{v} of the projections of $\mathbf{P}$ in the rotated camera. Finally, the depth d of $\mathbf{P}$ in the original camera can be obtained by

$$d = \frac{d_{\mathrm{v}}}{\cos\alpha_{\mathrm{v}}}\cos\alpha. \quad (10)$$

3.3. Recovering Pose of the Medium

It has been shown in the previous subsection that scene depth can be recovered given the orientation of the parallel planar faces of the transparent medium. In this subsection, we will show how the orientation of the parallel planar faces of the medium can be recovered directly from the displacements of the scene points in the images.

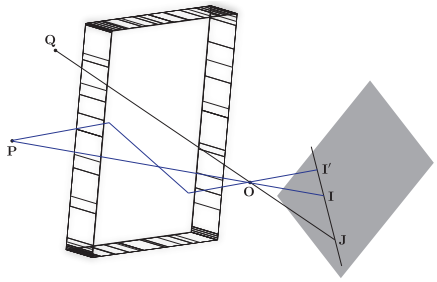

Figure 6. Recovering the orientation of the parallel planar faces of the transparent medium. A refraction line defined by corresponding points in the direct and refracted images contains the vanishing point for the normal direction of the parallel planar faces of the medium.

Consider a 3D point $\mathbf{Q}$ whose visual ray is perpendicular to the parallel planar faces of the medium (see Fig. 6). By construction, the visual ray of $\mathbf{Q}$ will simply pass straight through the medium without any change of direction. Hence, the projections of $\mathbf{Q}$ will be identical in both the direct image and refracted image. Let us denote this point by $\mathbf{J}$. Without loss of generality, consider another 3D point $\mathbf{P}$, and let $\mathbf{I}$ and $\mathbf{I}'$ be the projections of $\mathbf{P}$ in the direct image and the refracted image respectively. Referring to Section 2, the refraction plane of $\mathbf{P}$ is perpendicular to the parallel planar faces of the medium. Since this plane contains both $\mathbf{P}$ and $\mathbf{O}$, and that the ray $\mathbf{OQ}$ is, by construction, also perpendicular to the parallel planar faces of the medium, it follows that $\mathbf{Q}$ must also lie on this plane. This plane intersects the image plane along a line which we refer to as a *refraction line*. It is obvious that both $\mathbf{J}$, $\mathbf{I}$ and $\mathbf{I}'$ must lie on this line. Based on this observation, we have the following proposition:

Proposition 1. *Given the correspondences of two or more scene points in a direct image and a refracted image, the refraction lines defined by the correspondences will intersect at a single point which corresponds to the vanishing point for the normal direction of the parallel planar faces of the medium.*

The two corollaries below then follow directly from Proposition 1:

Corollary 1. *The orientation of the parallel planar faces of the transparent medium can be recovered as the visual ray for the point of intersection between two or more refraction lines defined by correspondences in the direct image and the refracted image.*

Corollary 2. *Given the projection* $\mathbf{I}$ *of a scene point* $\mathbf{P}$ *in the direct image, its correspondence* $\mathbf{I}'$ *in the refracted image must lie on the half-infinite line* $\mathbf{I}'(t) = \mathbf{I} + t(\mathbf{I} - \mathbf{J})$ *where* $t \geq 0$ *and* $\mathbf{J}$ *is the the vanishing point for the normal direction of the parallel planar faces of the medium.*

Having recovered the vanishing point $\mathbf{J}$ for the normal direction of the parallel planar faces of the medium from some correspondences, more correspondences can then be established with ease using the refraction line constraint derived from $\mathbf{J}$.

3.4. Estimation of the Refractive Index

In the previous discussions, we have assumed that the refractive index of the transparent medium is known. In this subsection, we will show the refractive index of the medium can be recovered from the displacements of scene points in three images.

Consider a 3D point $\mathbf{P}$. Let $\mathbf{I}$ be its projection in a direct image, and $\mathbf{I}'$ and $\mathbf{I}''$ be its projections in two refracted images captured with the transparent medium positioned in two different poses respectively. Let d be the depth of $\mathbf{P}$ estimated from $\mathbf{I}$ and $\mathbf{I}'$ using Eq. (10), and d' be the depth of $\mathbf{P}$ estimated from $\mathbf{I}$ and $\mathbf{I}''$ using Eq. (10). Now by equating d with d', the refractive index n of the medium can be recovered. In practice, given m pairs of correspondences in three images, the refractive index of the medium can be estimated by

$$n = \underset{n}{\operatorname{argmin}} \sum_{i=1}^{m} (d_i - d'_i)^2. \tag{11}$$

Note that a similar minimization can also be used to estimate the refractive index when there are more than two refracted images captured with the transparent medium positioned in different poses.

4. Experiment

The methods described in the previous sections for recovering the pose and refractive index of the medium, and the depth of the scene have been implemented. Experiments on both synthetic and real data were carried out and the results are presented in the following subsections.

4.1. Synthetic Experiment

Noise analysis was carried out in the case when the parallel planar faces of the medium were parallel to the image plane. Uniformly distributed random noise was added to the pixel coordinates with noise levels ranging from 0 to 3 pixels. For each noise level, 1000 independent trials were performed. The experimental setup consisted of some 3D points being viewed by a synthetic camera with a focal length of $70mm$. In the first experiment, the thickness of the medium was $4cm$ and its refractive index was 1.4. Experiments were carried out for distinct viewing angles. Fig. 7 (a) shows a plot of the root mean square (RMS) of the relative depth errors against different noise levels for different viewing angles. It is shown that for a particular noise level, depth accuracy could be improved by increasing the viewing angle in the case when medium surfaces

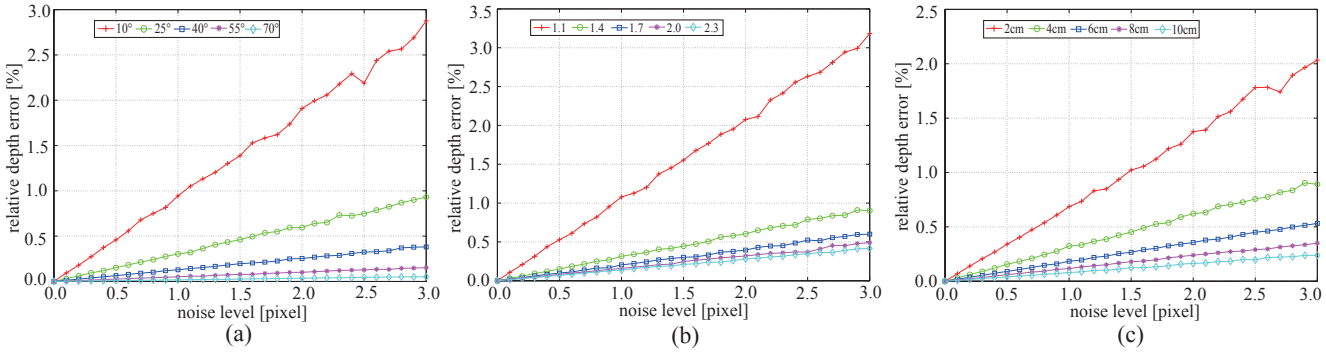

Figure 7. Depth accuracy can be improved in three ways: (a) increasing the angle between the visual ray and the surface normal of the medium; (b) increasing the refractive index; or (c) increasing the thickness of the medium.

are parallel to the image plane. In the general case, it implies that depth accuracy could be improved by increasing the angle between the visual ray and the surface normal of the medium. In the second experiment, the viewing angle and thickness of the medium were $25°$ and $4cm$, respectively. Experiments were performed for different refractive indices. Fig. 7 (b) shows a plot of the RMS of the relative depth errors against different noise levels for different refractive indices. It is shown that for a particular noise level, depth accuracy could be improved by increasing the refractive index. For a refractive index of 1.4, the relative depth error is less than 1.0% under a 3-pixel noise level. In the third experiment, the viewing angle and refractive index of the medium were $25°$ and 1.4, respectively. Experiments were performed for different thicknesses of the medium. It is shown in Fig. 7 (c) that for a particular noise level, depth accuracy could be improved by increasing the thickness of the medium.

In the synthetic experiment of estimating the orientation of the parallel planar faces of the medium, a bunny model was captured using a synthetic camera and a $4cm$ thick transparent medium with a refractive index of 1.4. Noise with levels ranging from 0 to 3 pixels were added to the pixel coordinates of 8171 points. For each noise level, 100 independent trials were performed. The orientation of the parallel planar faces of the medium and the 3D coordinates of all the points were obtained using correspondences in the direct image and the refracted image. Fig. 8 (a) shows the RMS angular error of the estimated normal of the parallel planar faces, as well as the RMS of the relative depth errors against different noise levels. The reconstruction result with a noise level of 1.0 pixel is shown in Fig. 8 (c, d).

In the synthetic experiment of estimating the refractive index of the medium, a third image of the bunny model was captured with the transparent medium positioned in a different pose. The orientations of the parallel planar faces of the medium were estimated using correspondences between the direct image and each of the two refracted images. The refractive index of the medium and the 3D coordinates of all the points were then obtained using correspondences in all three images. Fig. 9 (a) shows the RMS error of the estimated refractive index and the RMS of the relative depth errors against different noise levels. The reconstruction result with a noise level of 1.0 pixel is shown in Fig. 9 (c,d).

4.2. Real Experiment

A common transparent glass (i.e., it is not of optical grade) with parallel planar faces and a thickness of $4.9cm$ (measured by a common ruler) was used in all the real experiments. In fact, it follows from Eq. (8) that if the thickness is unknown, the shape could also be obtained up to a scale. In the first real experiment, one direct image and two refracted images of a model building were captured by a camera. The intrinsic parameters of the camera were calibrated using [2]. Correspondences of the corners on the surface of the model were picked manually. The direct image of the model with corners marked by red crosses is shown in Fig. 10 (a). More correspondences among the three images were obtained by SIFT feature matching [8]. SIFT was first performed to obtain matches between the direct image and the first refracted image. RANSAC [5] was then used to eliminate outliers. In using RANSAC, two pairs of matches were sampled to recover the orientation of the parallel planar faces of the medium as the intersection of the two refraction lines defined by the correspondences, and inliers were identified by computing the distance of the intersection point from the refraction lines defined by each pair of correspondences. The same procedure was performed to obtain correspondences between the direct image and the second refracted image. The matches among three images were then obtained by combining correspondences between images. The poses and the refractive index of the medium, and the 3D coordinates of the points were estimated using all the correspondences (obtained manually and by SIFT) among three images. The model building generated using the reconstructed corners is shown in Fig. 10 (b, c).

The experimental results were also quantitatively compared against those obtained using a calibration pattern in

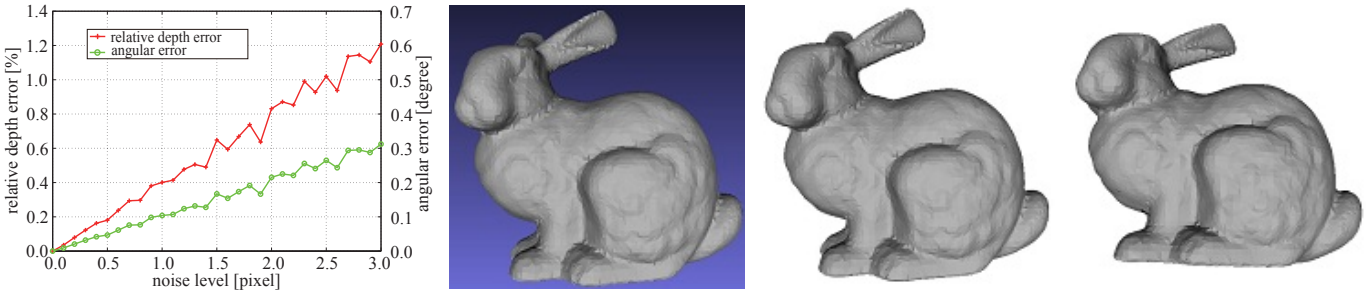

(a) (b) (c) (d)

Figure 8. Reconstruction of the bunny using a direct image and a refracted image. (a) Estimation of the orientation of the parallel planar faces of the medium and the depths of points on the surface of the bunny model; (b) the original bunny model; (c, d) two views of the reconstructed bunny model.

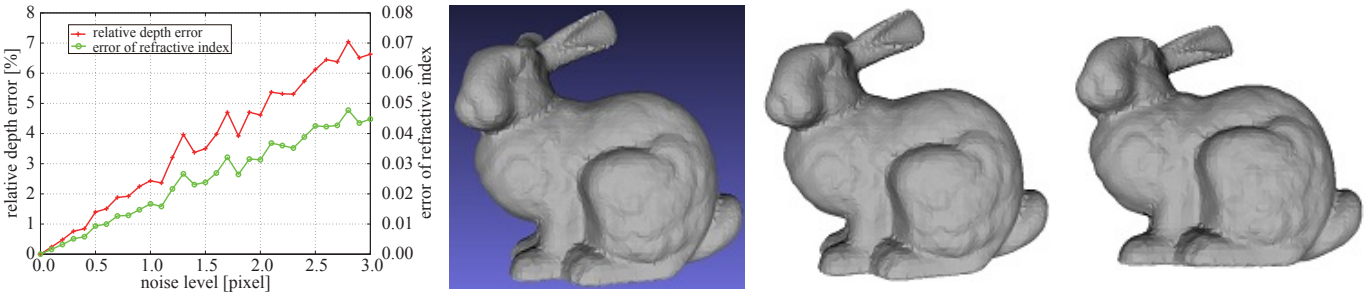

(a) (b) (c) (d)

Figure 9. Reconstruction of the bunny using a direct image and two refracted images captured with the transparent medium in two different poses. (a) Estimation of the refractive index of the medium and the depth of points on the surface of the bunny model; (b) the original bunny model; (c, d) two views of the reconstructed bunny model.

[3], which were treated as the ground truth. In the experiment, depth of each corner in the pattern could be computed by taking a direct image of the calibration pattern. The ground truth of the first orientation of the medium and the refractive index could then be estimated by using the depths of the corners in the pattern. After calibration, the model building was placed in the view of the camera without moving the camera and medium. The angle between the estimated normal of the medium and the ground truth is $4.05°$. The ground truth refractive index is 1.438, and the estimated index is 1.435. The reconstructed 3D points were re-projected to the three images. The RMS of the re-projection errors is 0.726 pixel.

In the second real experiment, one direct image and one refracted image were used to obtain the depth map of the scene. The orientation of the medium surface was estimated from the correspondences in two images obtained using SIFT. SIFT flow [7] was then used to obtain dense correspondences across the two images. From the dense correspondences, our method can recover a high-precision result of a cat model, as shown in Fig. 11. Fig. 12 shows the result of a more complicated scene recovered using the same procedure. Note that the artifacts in both figures were caused by the inaccuracy of correspondences obtained by SIFT flow method.

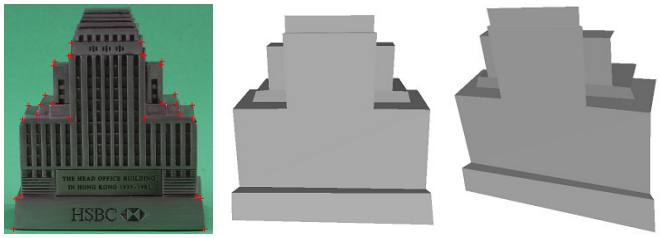

(a) (b) (c)

Figure 10. Reconstruction of a model building. (a) A direct image of the model with corners marked by red crosses; (b,c) two views of the reconstructed model.

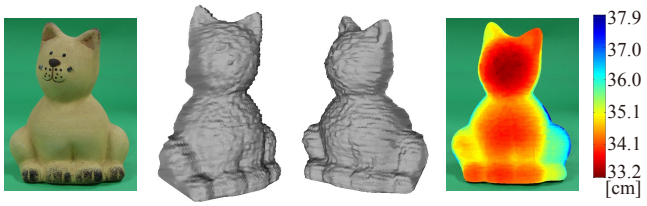

(a) (b) (c) (d)

Figure 11. The reconstruction result of a model cat. (a) A direct image; (b, c) two views of the reconstructed cat model; (d) depth map of the model.

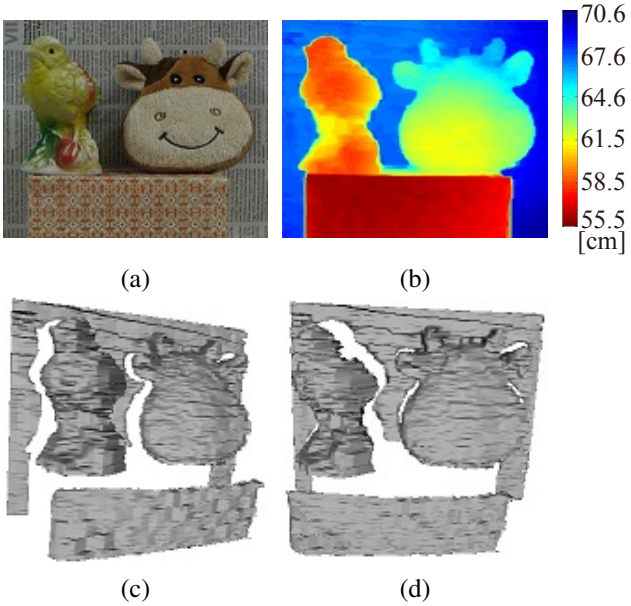

Figure 12. The reconstruction result of a scene consisting of two toy models. (a) A direct image; (b) depth map of the scene; (c, d) two views of the reconstructed scene.

5. Conclusions

A self-calibrating depth from refraction method is introduced in this paper. It is demonstrated that a transparent medium with parallel planar faces can be used to recover scene depth. Two images of a scene are captured by a camera with and without placing a transparent medium between the scene and the camera. Correspondences in images are then used to obtain the orientation of the parallel planar faces of the medium and the depths of scene points. It is further pointed out that a third image with the medium positioned in another orientation could be used to estimate the refractive index of the medium. Experiments on both synthetic and real data show promising results. With the proposed method, the pose and refractive index of the transparent medium, and depths of scene points can be estimated simultaneously. Nevertheless, the proposed method suffers from the same intrinsic limitation as other existing depth from refraction methods: it corresponds to a small baseline multi-view approach. Hence the proposed method could only be used to recover depth for close scenes.

References

[1] S. Agarwal, S. P. Mallick, D. Kriegman, and S. Belongie. On refractive optical flow. In *Proc. European Conf. on Computer Vision*, pages 483–494, 2004. 2

[2] J.-Y. Bouguet. Camera calibration toolbox for matlab. http://www.vision.caltech.edu/bouguetj/calib_doc/. 6

[3] C. Gao and N. Ahuja. Single camera stereo using planar parallel plate. In *Proc. Int. Conf. on Pattern Recognition*, volume 4, pages 108–111, 2004. 2, 7

[4] C. Gao and N. Ahuja. A refractive camera for acquiring stereo and super-resolution images. In *Proc. Conf. Computer Vision and Pattern Recognition*, volume 2, pages 2316–2323, 2006. 2

[5] R. I. Hartley and A. Zisserman. *Multiple View Geometry in Computer Vision*. Cambridge University Press, second edition, 2004. 6

[6] D. Lee and I. Kweon. A novel stereo camera system by a biprism. *IEEE Transactions on Robotics and Automation*, 16:528–541, 2000. 2

[7] C. Liu, J. Yuen, and A. Torralba. Sift flow: Dense correspondence across scenes and its applications. *IEEE Trans. on Pattern Analysis and Machine Intelligence*, 2010. 7

[8] D. Lowe. Object recognition from local scale-invariant features. In *Proc. Int. Conf. on Computer Vision*, volume 2, pages 1150–1157, 1999. 6

[9] H.-G. Maas. New developments in multimedia photogrammetry. *Optical 3-D Measurement Techniques III*, 1995. 2

[10] N. Morris and K. Kutulakos. Dynamic refraction stereo. In *Proc. Int. Conf. on Computer Vision*, volume 2, pages 1573–1580, 2005. 2

[11] H. Murase. Surface shape reconstruction of a nonrigid transport object using refraction and motion. *IEEE Trans. on Pattern Analysis and Machine Intelligence*, 14:1045–1052, 1992. 2

[12] A. P. Pentland. A new sense for depth of field. *IEEE Trans. on Pattern Analysis and Machine Intelligence*, 9:523–531, 1987. 2

[13] S. M. Seitz, B. Curless, J. Diebel, D. Scharstein, and R. Szeliski. A comparison and evaluation of multi-view stereo reconstruction algorithms. In *Proc. Conf. Computer Vision and Pattern Recognition*, volume 1, pages 519–528, 2006. 2

[14] M. Shimizu and M. Okutomi. Reflection stereo - novel monocular stereo using a transparent plate. In *Proc. on Canadian Conference on Computer and Robot Vision*, pages CD–ROM, 2006. 2

[15] M. Shimizu and M. Okutomi. Monocular range estimation through a double-sided half-mirror plate. In *Proc. on Canadian Conference on Computer and Robot Vision*, pages 347–354, 2007. 2

[16] M. Shimizu and M. Okutomi. Calibration and rectification for reflection stereo. In *Proc. Conf. Computer Vision and Pattern Recognition*, pages 1–8, 2008. 2

[17] M. Subbarao and N. Gurumoorthy. Depth recovery from blurred edges. In *Proc. Conf. Computer Vision and Pattern Recognition*, pages 498–503, 1988. 2

[18] G. Surya and M. Subbarao. Depth from defocus by changing camera aperture: a spatial domain approach. In *Proc. Conf. Computer Vision and Pattern Recognition*, pages 61–67, 1993. 2

[19] C. Zhou, O. Cossairt, and S. Nayar. Depth from diffusion. In *Proc. Conf. Computer Vision and Pattern Recognition*, 2010. 2

[20] C. Zhou, S. Lin, and S. Nayar. Coded aperture pairs for depth from defocus. In *Proc. Int. Conf. on Computer Vision*, pages 325–332, 2009. 2